Published in final edited form as:
Clin Cancer Res. 2009 February 15; 15(4): 1192–1198. doi:10.1158/1078-0432.CCR-08-2150.

Combining the ER-stress inducing agents bortezomib and fenretinide as a novel therapeutic strategy for metastatic melanoma

David S. Hill[1], **Shaun Martin**[1], **Jane L. Armstrong**[2], **Ross Flockhart**[1], **Joge J. Tonison**[1], **Dominic G. Simpson**[1], **Mark A. Birch-Machin**[1], **Christopher P.F. Redfern**[2], and **Penny E. Lovat**[1]

[1]Dermatological Sciences, Institute of Cellular Medicine, Newcastle University, UK

[2]Northern Institute for Cancer Research, Newcastle University, UK

Abstract

Purpose—Single agent chemotherapy is largely the treatment of choice for systemic therapy of metastatic melanoma but survival rates are low and novel adjuvant and systemic therapies are urgently required. Endoplasmic reticulum (ER) stress is a potential therapeutic target and two relatively new drugs, fenretinide and bortezomib (Velcade®), each acting via different cellular mechanisms, induce ER stress leading to apoptosis in melanoma cells. The aim of this study was to test the hypothesis that apoptosis of melanoma cells may be increased by combining clinically-achievable concentrations of fenretinide and bortezomib.

Experimental Design—Three human melanoma cell lines were used to assess changes in viability and the induction of apoptosis in response to fenretinide, bortezomib, or both drugs together. A subcutaneous xenograft model was used to test responses *in vivo*.

Results—Fenretinide and bortezomib synergistically decreased viability and increased apoptosis in all three melanoma lines at clinically-achievable concentrations. This was also reflected by increased expression of GADD153, a marker of ER stress-induced apoptosis. *In vivo*, fenretinide in combination with bortezomib gave a marked reduction in xenograft tumor volume and increase in apoptosis compared with fenretinide or bortezomib alone. The cell cycle stage of tumor cells *in vivo* were similar to that predicted from the effects of each drug or the combination *in vitro*.

Conclusions—These results suggest that fenretinide and bortezomib, both of which are available in clinical formulation, warrant clinical evaluation as a combination therapy for metastatic melanoma.

Cutaneous malignant melanoma, the most aggressive form of skin cancer, is one of the most difficult forms of human cancer to treat with an increasing incidence in developed countries which has risen faster than any other malignancy over the past 40 years (1). Improvements in early detection and surgical management of early stage disease have resulted in cure for most patients with primary melanoma (1, 2). However, advanced metastatic melanoma is highly invasive and has the capacity to develop resistance to drug-induced apoptosis and host immunological defences (1). Single agent chemotherapy remains largely the treatment of choice for systemic therapy of metastatic melanoma (3). Dacarbazine (DTIC), temozolomide and fotemustine are widely used because of their low toxicity and simplicity

Requests for Reprints: Dr Christopher Redfern, Northern Institute for Cancer Research, Newcastle University Paul O'Gorman Building, The Medical School, Newcastle upon Tyne NE2 4HH UK Tel: +44 191 2224416 chris.redfern@ncl.ac.uk.
D.S. Hill and S. Martin are joint first authors; C.P.F. Redfern and P.E. Lovat are joint senior authors.

Europe PMC Funders Author Manuscripts

of administration; more-toxic combination therapies do not improve survival (1). Other chemotherapies including cisplatin and paclitaxel have shown some activity but, despite clinical trials of differing combinations of chemotherapeutic agents, none have proved superior to single agent DTIC. Since DTIC still only yields a response rate of 16% which is rarely sustained beyond 6 months (1), other therapeutic approaches combining immunotherapy with either interleukin (IL)-2 or interferon (IFN) alpha with DTIC (or temozolomide and fotemustine) have been tried (1, 4). However, although initial response rates were slightly improved, these regimes have not been associated with better overall survival. Furthermore, administration of either IL-2 or IFN has multiple adverse side effects(1). Hence, overall, little progress has been made towards an effective treatment for metastatic melanoma and with median survival rates rarely exceeding 12 months in clinical trials, novel adjuvant and systemic therapies are urgently required.

Melanoma cells are frequently resistant to apoptosis induced by conventional mechanisms of death receptor ligation (5) or mitochondrial-mediated apoptosis (6, 7). It has been suggested that the activation of endoplasmic reticulum (ER) stress is an important factor limiting melanoma progression (8) and recent studies have shown that the induction of apoptosis resulting from endoplasmic reticulum stress may offer novel therapeutic strategies for metastatic melanoma (9, 10). We have recently shown that bortezomib, a 26S proteasome inhibitor, and fenretinide, a synthetic derivative of retinoic acid, induce ER stress culminating in apoptosis of metastatic melanoma cell lines *in vitro* (10). Although the efficacy of bortezomib as a single agent appears limited (11), pre-clinical studies suggest that the chemosensitivity of metastatic melanoma to bortezomib may be increased in combination with temozolomide (12). Bortezomib may also sensitize cancer cells to apoptosis induced by other ER stress-inducing agents (13). In A375 melanoma cells, fenretinide induces ER stress and apoptosis via oxidative stress whereas bortezomib induces ER stress by a different mechanism (9). Evidence from in vitro studies suggests that metastatic cells are sensitive to fenretinide (14) and this retinoid may be a valuable agent for cancer prevention and treatment. However, clinical studies of fenretinide in melanoma have shown little efficacy (15). Since fenretinide and bortezomib may induce ER stress in metastatic melanoma cells via different mechanisms, the aim of this study was to test the hypothesis that the combination of fenretinide and bortezomib would be a more effective strategy for the clinical use of these agents for metastatic melanoma.

Materials and Methods

Cell Culture, Drug Treatment and analysis of cell viability and apoptosis *in vitro*

Human metastatic melanoma cell lines CHL-1, A375 and WM266-4 were from the American Type Culture Collection (Teddington, UK) and cultured as previously described (10). Fenretinide (Janssen-Cilag Ltd, Basserdorf, Switzerland), temozolomide (OSI Pharmaceuticals), bortezomib (Velcade®; Janssen-Cilag Ltd, High Wycombe, UK) or thapsigargin (Sigma Chemical Co, Poole, UK) were added in ethanol (fenretinide) or DMSO (temozolomide, bortezomib or thapsigargin) with an equal volume of vehicle used to treat control cells. Flow cytometry of propidium-iodide-stained cells was used to estimate the level of cell death or apoptosis by measuring the percentage of cells in the sub-G1 fraction (9). Cell cycle analysis was done using Modfit LT v3.1 (Verity Software House, Topsham, ME) to estimate the proportion of cells in G0+G1 and G2+M, using a 6-compartment S-phase model, including aggregates and debris, applied to cells gated within an ellipse (long axis G0+G1 peak to G2+M peak) enclosing the G0+G1 to G2+M populations). Cell viability was measured using commercial MTS assay (CellTiter 96® AQueous Assay; Promega, Southampton,UK) according to the Manufacturer's protocol.

Western Blotting

Total protein was extracted from cell pellets, separated by electrophoresis through 4-20% SDS-PAGE gels (20 μg per track) and blotted onto PVDF membranes as previously described (9). Blots were probed with an antibody to GADD153 (Santa Cruz Biotechnology, B-3; Autogen Bioclear, Calne, UK) diluted 1:500, and, as a loading control, with a β-actin antibody (Sigma) diluted 1:5000. The binding of primary antibodies was detected with secondary peroxidase-conjugated antibodies (Upstate Biotechnology, Watford, UK) diluted 1:2000 and visualized using the ECL system (Amersham Biosciences, Amersham, UK).

Xenograft mouse model

Female CD1 nude mice, 6-8 weeks old (Charles River, East Lothian, UK), were inoculated subcutaneously into the right flank with 7.5×10^6 A375 cells in 100 μl DMEM containing 4.5 g/L L-Glucose (BioWhittaker, Lonza, Verviers, Belgium). On establishment of tumors 125 mm^3 in volume, mice were randomised into 4 treatment groups (6 mice per group) and treated subsequently by daily intravenous injection (tail) for 10 days with 1.45 mg/kg fenretinide or 0.1 mg/kg bortezomib or the combination of both agents. The control group were treated with 100 μl of diluent only (DMEM containing 4.5 g/L glucose). Calliper measurements of tumor length (L) and width (W) were taken every day and tumor volume determined using the formula V= ((L*L)*W)/2. Mice were humanely killed on the final day of treatment and tumors extracted and snap frozen in liquid nitrogen prior to storage at −80°C and subsequent histological analysis.

Immunohistochemistry

Analysis of tumors from animals treated with fenretinide, bortezomib or the combination of both agents was performed by immunohistochemistry of frozen tissue sections (16). Frozen sections (6 μm) prepared on (3-Aminopropyl)triethoxysilane (APES, Sigma)-coated glass slides were fixed in ice-cold acetone for 10 min prior to staining with a Ki67 antibody or 4% paraformaldehyde prior to staining by terminal deoxynucleotidyl transferase-mediated dUTP-X nick end labelling (TUNEL). After permeabilisation for 10 min with 0.2% Triton-X (Sigma) in phosphate buffered saline (PBS), two washes with PBS containing 0.05% tween 20 (PBS/T, Sigma), sections were immersed in 10% goat serum in PBS/T for 10 min to minimise non-specific binding before treatment with a rabbit anti-Ki67 antibody (Novocastra Laboratories Ltd, Newcastle upon Tyne, UK) diluted 1:300 in PBS/T for 1 h at room temperature. Ki67 staining was detected with a secondary fluorescein isothiocyanate-conjugated goat anti-rabbit secondary antibody (Invitrogen Ltd, Paisley, UK) diluted 1:200 in PBS/T containing 2% bovine serum albumin (BSA, Sigma) for 1 h at room temperature before counterstaining nuclei for 15 min with TOTO-3 iodide (Invitrogen) diluted 1:7,000 in PBS/T containing 2% BSA. Stained sections were mounted in Vector Shield (Vector Laboratories, Peterborough, UK) and analysed by confocal microscopy using a Leica TCS SP II laser scanning confocal microscope with images captured and processed using LCS Lite 2.61 software (Leica Microsystems, Heidelberg, Germany). Tumors were processed for TUNEL staining in the same way and detected using a commercial kit (Roche Diagnostics, Mannheim, Germany) according to the Manufacturer's specifications.

To assess changes in cell cycle parameters *in vivo*, tumor sections (prepared as above) were stained with methylene blue (17) to measure nuclear area. After a 5 min wash in distilled water and 30 s rinse in 1 mol/L hydrochloric acid, sections were incubated at 60 °C in 1 mol/L HCl for 10 min followed by further washes in distilled water and 1 mol/L HCl each for 30 s prior to incubation in Schiff's reagent for 1 h (Sigma). After washing 3 times with sulphite rinse (50 mmol/L HCl containing 6% aqueous sodium metabisulfite) for 2 min each, sections were stained with 0.5% methylene blue (BDH, Poole, Dorset) for 10 s at room temperature, dehydrated though 100% ethanol, cleared in Histo-Clear II solution (Raymond

Lamb Ltd, Sussex, UK) and mounted in DPX (Raymond Lamb). Staining was visualised by light microscopy and images captured and analysed using Leica QWin software (Leica Microsystems, Heidelberg, Germany).

Statistical analysis

For the analysis of responses to combined treatment of melanoma cells *in vitro*, the CalcuSyn program (Biosoft, Cambridge, UK) was used to derive parameter estimates for the median-effect equation with single drug treatments (fenretinide or bortezomib) and combination indices for combined treatments: combination index values around 1 indicate additivity, <1 synergy and >1 inhibition (18). For cell cycle data, G0+G1/G2+M ratios, referred to here as G1/G2 ratio, were analysed after log transformation to equalise the variances (Log10[1+G1/G2]) by SPSS Release 15 (SPSS Inc., Chacago, Il); transformed values were analysed by drug treatment separately (fenretinide, bortezomib, or the combination) using two-way ANOVA (cells, drug dose), one-way ANOVA with Dunnett's post-hoc test to compare with control treatments and by General Linear Models (GLM) on drug-treated cells using cell type as factor and drug dose as a covariate. In the xenograft experiment, tumor volumes were expressed as relative to day 1. For analysis of final relative tumor volumes, the data were log-transformed to equalise variances and tested for normality using a 1-sample Kolmogorov-Smirnoff (Lillefors) test (P>0.05); these data were analysed conservatively by one-way ANOVA using Bonferroni correction for post-hoc pairwise comparisons. For analysis of Ki67 and TUNEL staining, image analysis was performed using Velocity version 4.3.1 (Improvision Ltd, Coventry, UK). Nuclei were defined using the fluorescent intensity of the nuclear marker dye (TOTO-3) and applying appropriate thresholding and size exclusion filters. For each nucleus, the fluorescence value and mean fluorescent intensity for TUNEL or Ki-67 from each image was recorded. Percentage change in positivity was determined by setting a threshold value on the negative control for each analysis (kept constant between analyses). The same threshold value was set on drug-treated samples so that the change in nuclear positivity was normalised to the untreated control. For each tumor (6 animals per treatment group), values were reported as the mean percentage of positive nuclei from three independent staining analyses (a total of ≥ 12 images and ≥ 2100 cells per treatment). For analysis of methylene blue staining, the mean nuclear area from 200 nuclei was derived using Leica QWin. Values were reported as the means from 4 independent staining analyses for each treatment group (n=6 per group). Results from all immunocytochemical analyses were compared by one-way ANOVA with Dunnett's post-hoc test using SPSS Release 15.

Results

Fenretinide and bortezomib inhibit cell viability and induce apoptosis of metastatic melanoma cells in vitro

Bortezomib and fenretinide induce ER stress and apoptosis when added as single agents to CHL1, A375 and WM266-4 melanoma cells *in vitro* (10). The viability dose-response curves for fenretinide gave IC_{50} values of 14 (95% confidence range 10-20), 24 (12-47) and 25 (13-51) μmol/L for CHL-1, A375 and WM266-4 cells, respectively (Fig. 1); viability dose-response curves for bortezomib were shallower but with IC_{50} values of 0.1 (0.05-0.2), 0.4 (0.2-1) and 1.4 (0.7-2.6) μmol/L, for the respective cell lines. Thus, CHL-1 cells were more sensitive to these drugs than A375 or WM266-2 cells, with the latter showing greatest resistance to bortezomib. When fenretinide and bortezomib were added to melanoma cells in combination, there was a weak synergistic reduction in viability over fixed-ratio dose ranges of 2.5/0.05 to 20/0.4 μmol/L fenretinide/bortezomib (Combination Indices 0.305-0.73; Fig. 1). The decrease in viability in response to fenretinide or bortezomib was mirrored by an increase in apoptosis and for this measure of effect the combination of the two drugs was

weakly synergistic at fixed ratio doses at concentrations of 2.5/0.05 μmol/L to 5/0.1 μmol/L fenretinide/bortezomib (Combination Indices 0.3-0.84), but additive or weakly inhibitory at higher doses of 15/0.3-20/0.4 μmol/L fenretinide/bortezomib (Combination Indices 1-1.35). A375 cells showed the best apoptotic response to the drug combination *in vitro* with Combination Indices of 0.3-0.5 over the 2.5/0.05 to 10/0.2 μmol/L dose range.

Since bortezomib has been reported to induce G2/M arrest (19), the ratio of G0+G1/G2+M ratio (here referred to as G1/G2 ratio) in the cell lines was analysed for all drug treatments. Although the G1/G2 ratio was substantially reduced in all three cell lines (increased proportion of cells in G2) in response to bortezomib treatment compared to control, there was no dose-dependent relationship between bortezomib and decreased G1/G2 ratio (Fig. 1). The greatest G2/M arrest in response to bortezomib was obtained in CHL1 cells with the least effect obtained in A375 cells (Fig. 1). In contrast to bortezomib, there was no change in G1/G2 ratio in A375 cells in response to fenretinide (one-way ANOVA, Dunnett's, $P>0.3$), but an increase in G1/G2 ratio (greater proportion of cells in G1) in CHL-1 and WM266-4 cells treated with fenretinide at 10-20 μmol/L (CHL-1 cells) or 20 μmol/L (WM266-4 cells). In these two cell lines, the data suggest a dose-dependent effect of fenretinide (Fig. 1). For cells treated with bortezomib and fenretinide together at a constant dose ratio, there was a linear, dose-dependent increase in G1/G2 ratio and significant differences between cells (Fig.1). These results suggest that in the presence of both drugs, a bortezomib-induced G2/M arrest predominates at low fenretinide doses but increased levels of apoptosis at higher fenretinide concentrations results in a relative decrease in cells in G2/M.

Expression of GADD153 is characteristic of the ER-stress mediated apoptosis pathway (20) and was therefore used as a marker of an increased ER-stress response in melanoma cells in response to drug combinations. Fenretinide or bortezomib as single agents induced GADD153 in CHL-1 cells but induction was weaker or barely detectable in A375 and WM266-4 melanoma cells (Fig. 2). For these experiments, fenretinide and bortezomib were used at concentrations of 10 μmol/L and 0.2 μmol/L, respectively; at these concentrations of each drug alone the decrease in viability or increase in apoptosis, relative to control cells, was small (Fig. 1) and this is also reflected by the low level of GADD153 induction at these doses. However, when fenretinide and bortezomib were used in combination at these doses, there was a marked induction of GADD153 (Fig. 2) in all three cell lines. In these experiments, thapsigargin, an ER stress inducer (9), and temozolomide, a DNA-damaging alkylating agent (21), were used as positive and negative controls, respectively. These results suggest that the synergistic induction of apoptosis and decrease in viability in response to fenretinide and bortezomib in combination is a result of synergy in the ER stress-apoptosis pathway.

Effective inhibition of melanoma growth in vivo by fenretinide and bortezomib in combination

Our observation that, *in vitro*, fenretinide and bortezomib were synergistic suggests that these drugs in combination may be effective in controlling melanoma growth *in vivo*. The previous data show that A375 cells were relatively resistant to fenretinide or bortezomib as single agents; since A375 cells also carry the $BRAF^{V600E}$ activating mutation (22) and activating mutations in BRAF are characteristic of over 70% of human melanomas (23), this cell line was used to test the hypothesis that fenretinide and bortezomib will be effective in controlling melanoma growth in vivo using a subcutaneous xenograft model. Once tumors were established, daily treatment for 10 days with fenretinide, bortezomib, fenretinide and bortezomib or control vehicle was initiated. Treatment with fenretinide and bortezomib together resulted in almost complete cessation of tumor growth. At the end of the experiment, relative tumor volumes in animals treated with fenretinide and bortezomib together were significantly lower than in control animals, or in animals treated with

fenretinide or bortezomib alone (Fig. 3; $F_{3,20}$=12.42, P<0.0001; fenretinide and bortezomib compared to other treatments, P<0.004). Tumor volumes in animals treated with fenretinide or bortezomib alone were not significantly different from control (P>0.65).

Tumors removed from the animals at sacrifice were processed for immunohistochemistry and tumor sections stained for proliferative activity (Ki67) and the presence of apoptotic cells (TUNEL). In addition, since bortezomib induced G2/M arrest in all three melanoma lines *in vitro*, sections were stained for DNA (methylene blue) to measure nuclear area as evidence of G2/M arrest *in vivo*. Proliferative activity, expressed as the percentage of Ki67-positive cells, was not significantly different between treatments (One-way ANOVA, $F_{3,20}$=1.773, P=0.185; Fig. 4). Conversely, the extent of apoptosis (percentage TUNEL-positive cells) differed significantly between treatments (One-way ANOVA, $F_{3,20}$=285.4, P<0.001) and was higher than control in tumors from animals treated with bortezomib (Dunnett's, P=0.004) and was substantially higher than control and the bortezomib-only treatments in tumors from animals treated with fenretinide and bortezomib together (Dunnett's, and bortezomib versus fenretinide plus bortezomib contrast, P<0.001;Fig. 4). The mean nuclear area of tumor cells differed significantly between treatment groups (One-way ANOVA, $F_{3,20}$=24.33, P<0.001) and in tumors from animals treated with bortezomib alone (Dunnett's, P<0.001) was approximately twice that in tumors from the other treatments, consistent with bortezomib-induced G2 arrest. The mean nuclear areas in tumors from the fenretinide or the combined fenretinide and bortezomib treatments were not significantly different from control (Dunnett's, P> 0.13; Fig. 4). Therefore, with respect to the combination treatment, these *in vivo* results mirror the *in vitro* data in which the bortezomib-induced accumulation of cells in G2/M was counteracted by increased apoptosis in response to fenretinide or both drugs acting together.

Discussion

The results from this study show that fenretinide and bortezomib were synergistic at concentrations within the lower range of their dose-response curves for the induction of apoptosis and throughout the concentration range for decreased viability. The three cell lines used differed in their sensitivity to fenretinide or bortezomib, but showed similar levels of synergy with respect to decreased viability when the drugs were used in combination. As in studies on other cell types (24, 25), bortezomib induced G2/M arrest in all three melanoma cell lines, even at the lowest doses used (0.05 μmol/L). There was no evidence for dose-dependency in G2/M arrest and the apoptotic dose-response curves for bortezomib were relatively shallow in all three cell lines. Since apoptosis was assessed by relative DNA content of sub-G1 cells, cells entering apoptosis from G2 would not be included and the total apoptosis in response to bortezomib may be underestimated. However, viability dose-response curves for bortezomib were also relatively shallow and it is likely that a G2/M arrest is the main outcome of bortezomib treatment over a short timescale *in vitro*.

In contrast to bortezomib, fenretinide gave steep dose-response curves for the induction of apoptosis in the range 10-15 μmol/L and produced a dose-dependent increase in the proportion of cells in G1 in CHL1 and WM266-4 cells. The combination of drugs showed a markedly linear decrease in the proportion of cells in G2/M with increasing constant-ratio doses of fenretinide and bortezomib and this may be an effect of increased fenretinide concentrations, perhaps preferentially inducing apoptosis in cells arrested in G2/M. The different effects on cell cycle parameters shown by fenretinide or bortezomib may reflect their different modes of action: unlike bortezomib, fenretinide induces oxidative stress leading to ER stress in melanoma cells (9). Conversely, bortezomib is a proteasome inhibitor with effects on a range of cellular signalling pathways. Bortezomib-induced G2/M arrest is associated with altered levels of the cell cycle regulators $p21^{WAF1}$, $p27^{Kip1}$, Cyclin B1,

CDK2, CDK4 and E2F4 in glioma cells (24), but the mechanism of bortezomib-mediated G2/M arrest is unknown. The proteasome is also a key component of the ER-associated degradation pathway which clears misfolded or excess proteins from the ER and is induced as part of the unfolded protein response (UPR) (26). Inhibiting this process leads to ER stress (27, 28) and increases ER stress resulting from other ER stress inducers (28). This mechanism is likely to underlie the synergy between fenretinide and bortezomib *in vitro* and *in vivo* and gives additional weight to studies suggesting that the most effective use of bortezomib will be in combination with drugs aimed at additional cellular targets (29).

Synergy between fenretinide and bortezomib was also apparent *in vivo*, as shown by the markedly reduced growth of subcutaneous A375 xenografts. Evidence that these drugs were working *in vivo* in a similar manner to that observed *in vitro* was provided by the histological analyses of the xenograft tumors; these were in agreement with predictions from *in vitro* data with respect to the induction of apoptosis, the accumulation of cells in G2/M in response to treatment with bortezomib alone and the abrogation of G2/M arrest by fenretinide and bortezomib used in combination. The synergy between fenretinide and bortezomib at the concentrations used *in vitro* and *in vivo* is important: pharmacokinetic studies of fenretinide and bortezomib in a variety of clinical settings define the plasma concentration of each drug achievable in patients. For fenretinide, low toxicity allows high doses to be ingested and the amount of drug delivered orally is mainly limited by the high number of capsules that need to be taken; mean peak plasma concentrations up to 13 μmol/L are achieved in children and adult cancer patients (30, 31) with steady state levels in the range 0.9-10 μmol/L (30, 32). Peak plasma concentrations of bortezomib up to 0.5 μmol/L can be achieved at appropriate doses (33-35) with biological half-lives of around 12 h (34-36). The present study on melanoma cell lines *in vitro* show that, for cell viability and apoptosis, fenretinide and bortezomib were synergistic at concentrations clinically-achievable in cancer patients: 2.5-10 μmol/L for fenretinide and 0.05-0.2 μmol/L bortezomib.

Clearly, although bortezomib has shown no evidence of clinical efficacy in metastatic melanoma on its own (11), on the basis of these results, combining bortezomib with fenretinide may be an effective therapeutic strategy. It is particularly pertinent that many tumor cells already have activated ER stress responses and display greater sensitivity to agents that increase ER stress still further, providing a mechanism to target tumor cells while minimising the damage to normal cells. Furthermore, while combining bortezomib with an additional ER stress inducer such as fenretinide, HDAC inhibitors (28), or inhibitors of ER stress recovery mechanisms (10) may be effective strategies, inhibiting downstream anti-apoptotic elements of the Bcl2 family proteins also increases apoptosis of melanoma cells in response to bortezomib (37). This raises the possibility that drug cocktails of fenretinide and bortezomib with clinically-available Bcl2-family inhibitors such as (-)-gossypol (37), or newer inhibitors in development such as ABT-737 (38), will be an exciting development for melanoma therapy.

Statement of Translational Relevance

Single agent chemotherapy is largely the treatment of choice for systemic therapy of metastatic melanoma but survival rates are low and novel adjuvant and systemic therapies are urgently required. Endoplasmic reticulum (ER) stress has emerged as a potential therapeutic target and two relatively new drugs, fenretinide and bortezomib (Velcade®), each acting via different cellular mechanisms, induce ER stress leading to apoptosis in melanoma cells. The results of this study show that apoptosis of melanoma cells *in vitro* and *in vivo* may be increased by combining clinically-achievable concentrations of fenretinide and bortezomib and that the effects of these drugs are

synergistic when used together. Fenretinide and bortezomib are both available in clinical formulations and this study suggests that clinical evaluation as a combination therapy for metastatic melanoma would be worthwhile.

Acknowledgments

Grant Support: Cancer Research UK, British Skin Foundation, Newcastle Health Care Charity. The authors thank R Stewart and C G Huggins for their technical assistance.

References

1. Thompson JF, Scolyer RA, Kefford RF. Cutaneous Melanoma. Lancet. 2005; 365:687–701. [PubMed: 15721476]
2. Rass K, Tilgen W. Treatment of melanoma and non melanoma skin cancer. Adv Exp Med Biol. 2008; 624:296–318. [PubMed: 18348465]
3. Atallah E, Flaherty L. Treatment of metastatic maliganant melanoma. Current Treatment Options in Oncology. 2005; 6:185–93. [PubMed: 15869730]
4. Quirt I, Verma S, Petrella T, Bak K, Charette M. Temozolomide for the treatment of metastatic melanoma: a systemic review. Oncologist. 2007; 12:1114–23. [PubMed: 17914081]
5. Xiao C, Yang BF, Song JH, Schulman H, Li L, Hao C. Inhibition of CaMKII-mediated c-FLIP expression sensitizes malignant melanoma cells to TRAIL-induced apoptosis. Exp Cell Res. 2005; 304:244–55. [PubMed: 15707589]
6. Karst AM, Dai DL, Martinka M, Li G. PUMA expression is significantly reduced in human cutaneous melanomas. Oncogene. 2005; 24:1111–6. [PubMed: 15690057]
7. Piro LD. Apoptosis, Bcl-2 antisense, and cancer therapy. Oncology. 2004; 18:5–10. [PubMed: 15651171]
8. Denoyelle C, Abou-Rjaily G, Bezrookove V, et al. Anti-oncogenic role of the endoplasmic reticulum differentially activated by mutations in the MAPK pathway. Nat Cell Biol. 2006; 8:1053–63. [PubMed: 16964246]
9. Corazzari M, Lovat PE, Armstrong JL, et al. Targeting homeostatic mechanisms of endoplasmic reticulum stress to increase suseptibility of cancer cells to fenretinide-induced apoptosis: the role of stress proteins ERdj5 and ERp57. Brit J Cancer. 2007; 96:1062–71. [PubMed: 17353921]
10. Lovat PE, Corazzari M, Armstrong JL, et al. Increasing melanoma cell death using inhibitors of protein disulphide isomerases to abrogate survival responses to endoplasmic reticulum stress. Cancer Res. 2008; 68:5363–9. [PubMed: 18593938]
11. Markovic SN, Geyer SM, Dawkins F, et al. A phase II study of bortezomib in the treatment of malignant melanoma. Cancer. 2005; 103:2584–9. [PubMed: 15887220]
12. Amiri KI, Horton LW, LaFleur BJ, Sosman JA, Richmond A. Augmenting chemosensitivity of maliganant melanoma tumors via proteosome inhibition: implication for Bortexomib (VELCADE, PS-341) as a therapeutic agent for malignant melanoma. Cancer Res. 2004; 64:4912–8. [PubMed: 15256463]
13. Nawrocki ST, Carew JS, Pino MS, et al. Bortezomib sensitizes pancreatic cancer cells to endoplasmic reticulum strss-mediated apoptosis. Cancer Res. 2005; 65:11658–66. [PubMed: 16357177]
14. Kadara H, Tahara E, Kim HJ, Lotan D, Myers J, Lotan R. Involvement of Rac in fenretinide-induced apoptosis. Cancer Res. 2008; 68:4416–23. [PubMed: 18519704]
15. Modiano MR, Dalton WS, Lippman SM, Joffe L, Booth AR, Meyskens FL Jr. Phase II study of fenretinide (N-[4-hydroxyphenyl]retinamide) in advanced breast cancer and melanoma. Invest New Drugs. 1990; 8:317–9. [PubMed: 2148744]
16. Al-Daraji WI, Grant KR, Ryan KM, Saxton A, N.J. R. Localization of calcineurin/NFAT in human skin and psoriasis and inhibition of calcineurin/NFAT activation in human keratinocytes by cyclosporin A. J Invest Dermatol. 2002; 118:779–88. [PubMed: 11982754]

17. Marconi G, Quintana R. Methylene blue dyeing of cellular nuclei during salpingoscopy, a new in-vivo method to evaluate vitality of tubal epithelium. Human Reprod. 1998; 13:3414–7.
18. Chou, T-C. The median-effect principle and the combination index for quantification of synergism and antagonism. In: Chou, T-C.; Rideout, DC., editors. Synergism and antagonism in chemotherapy. Academic Press; San Diego: 1991. p. 61-102.
19. Ling YH, Liebes L, Ng B, et al. PS-341, a novel proteasome inhibitor, induces Bcl-2 phosphorylation and cleavage in association with G2-M phase arrest and apoptosis. Mol Cancer Ther. 2002; 1:841–9. [PubMed: 12492117]
20. Oyadomari S, Mori M. Roles of CHOP/GADD153 in endoplasmic reticulum stress. Cell Death Differ. 2004; 11:381–9. [PubMed: 14685163]
21. Marchesi F, Turriziani M, Tortorelli G, Avvisati G, Torino F, De Vecchis L. Triazene compounds: mechanism of action and related DNA repair systems. Pharmacol Res. 2007; 56:275–87. [PubMed: 17897837]
22. Hoeflich KP, gray DC, Eby MT, et al. Oncogenic BRAF is required for tumor growth and maintenance in melanoma models. Cancer Res. 2006; 66:999–1006. [PubMed: 16424035]
23. Davies H, Bignell GR, Cox C, et al. Mutations of the BRAF gene in human cancer. Nature. 2002; 417:949–53. [PubMed: 12068308]
24. Yin D, Zhou H, Kumagai T, et al. Proteasome inhibitor PS-341 causes cell growth arrest and apoptosis in human glioblastoma multiforme (GBM). Oncogene. 2005; 24:344–54. [PubMed: 15531918]
25. Brignole C, Marimpietri D, Pastorino F, et al. Effect of bortezomib on human neuroblastoma cell growth, apoptosis, and angiogenesis. J Natl Cancer Inst. 2006; 98:1142–57. [PubMed: 16912267]
26. Kincaid MM, Cooper AA. ERADicate ER stress or die trying. Antioxid Redox Signal. 2007; 9:2373–87. [PubMed: 17883326]
27. Nawrocki ST, Carew JS, Dunner K Jr. et al. Bortezomib inhibits PKR-like endoplasmic reticulum (ER) kinase and induces apoptosis via ER stress in human pancreatic cancer cells. Cancer Res. 2005; 65:11510–9. [PubMed: 16357160]
28. Nawrocki ST, Carew JS, Pino MS, et al. Aggresome disruption: a novel strategy to enhance bortezomib-induced apoptosis in pancreatic cancer cells. Cancer Res. 2006; 66:3773–81. [PubMed: 16585204]
29. Kraus M, Malenke E, Gogel J, et al. Ritonavir induces endoplasmic reticulum stress and sensitizes sarcoma cells toward bortezomib-induced apoptosis. Mol Cancer Ther. 2008; 7:1940–8. [PubMed: 18645004]
30. Garaventa A, Luksch R, Piccolo MS, et al. Phase I trial and pharmacokinetics of fenretinide in children with neuroblastoma. Clin Cancer Res. 2003; 9:2032–9. [PubMed: 12796365]
31. Otterson GA, Lavelle J, Villalona-Calero MA, et al. A phase I clinical and pharmacokinetic study of fenretinide combined with paclitaxel and cisplatin for refractory solid tumors. Invest New Drugs. 2005; 23:555–62. [PubMed: 16034523]
32. Formelli F, Cavadini E, Luksch R, et al. Pharmacokinetics of oral fenretinide in neuroblastoma patients: indications for optimal dose and dosing schedule also with respect to the active metabolite 4-oxo-fenretinide. Cancer Chemother Pharmacol. 2008; 62:655–65. [PubMed: 18066548]
33. Attar EC, De Angelo DJ, Supko JG, et al. Phase I and pharmacokinetic study of bortezomib in combination with idarubicin and cytarabine in patients with acute myelogenous leukemia. Clin Cancer Res. 2008; 14:1446–54. [PubMed: 18316568]
34. Horton TM, Pati D, Plon SE, et al. A phase 1 study of the proteasome inhibitor bortezomib in pediatric patients with refractory leukemia: a Children's Oncology Group study. Clin Cancer Res. 2007; 13:1516–22. [PubMed: 17332297]
35. Ogawa Y, Tobinai K, Ogura M, et al. Phase I and II pharmacokinetic and pharmacodynamic study of the proteasome inhibitor bortezomib in Japanese patients with relapsed or refractory multiple myeloma. Cancer Sci. 2008; 99:140–4. [PubMed: 17970782]
36. Papandreou CN, Daliani DD, Nix D, et al. Phase I trial of the proteasome inhibitor bortezomib in patients with advanced solid tumors with observations in androgen-independent prostate cancer. J Clin Oncol. 2004; 22:2108–21. [PubMed: 15169797]

37. Wolter KG, Verhaegen M, Fernandez Y, et al. Therapeutic window for melanoma treatment provided by selective effects of the proteasome on Bcl-2 proteins. Cell Death Differ. 2007; 14:1605–16. [PubMed: 17541428]

38. Tagscherer KE, Fassl A, Campos B, et al. Apoptosis-based treatment of glioblastomas with ABT-737, a novel small molecule inhibitor of Bcl-2 family proteins. Oncogene. 2008

Europe PMC Funders Author Manuscripts

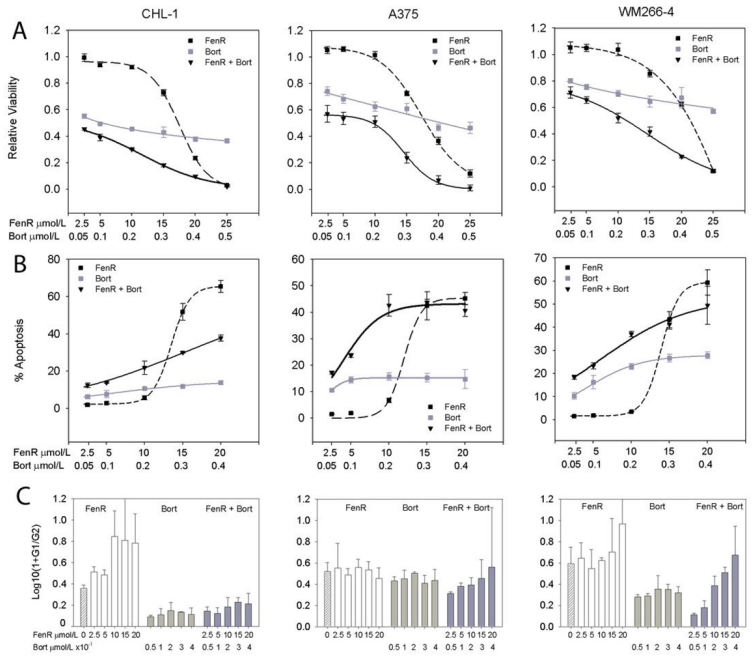

Figure 1.

Synergistic effects of fenretinide with bortezomib. Row *A*, viability (MTS assay) relative to control cells (Relative Viability); row *B*, % apoptosis and row C, the mean ratio (+95% confidence interval) of G0+G1 to G2+M cells (G1/G2) of CHL-1 (left column), A375 (centre column) and WM266-4 cells (right column) after 24 h treatment with fenretinide (FenR), bortezomib (Bort) or both agents combined at a fixed dose ratio of 50:1 (fenretinide:bortezomib). The highest doses used for the viability experiments were 25 μmol/L for fenretinide and 0.5 μmol/L for bortezomib, but apoptosis and cell cycle parameters were not analysed at these dose levels because the high levels of cell death made the measurements unreliable. In row *A* and *B*, each point is the mean of 8 replicates for viability and 3 for apoptosis experiments ± 95% confidence intervals. Sigmoidal curves (3- or 4-parameter) were fitted to the data using Sigmaplot (Systat Software Inc., San Jose, CA). In row C, the data were derived from flow cytometry analysis of PI-stained cells and expressed as the transformation Log10(1+G1/G2) (Ordinate). Bar heights are means + 95% confidence intervals. The hatched bars (first bar in each graph) in row C are data for control cells; open bars, fenretinide treatment; light gray bars, bortezomib; dark gray bars, fenretinide and bortezomib combined. Bortezomib substantially reduced the G1/G2 ratio in all three cell lines (one-way ANOVA, Dunnett's test, compared to control, $P<0.001$ for CHL1 and WM266-4 cells and for A375 cells $P\leq0.05$ for all except the 0.2 μmol/L treatment) but there was no dose-dependent relationship (GLM: $F_{5,39}=132$, $P<0.001$; main effect cell type $F_{2,39}=101$, $P<0.001$, but dose [excluding control; covariate term] and the cell-type*dose interaction terms were non-significant, $F<1.94$, $P>0.15$). The effect of fenretinide was dose dependent (GLM for CHL-1 and WM266-4 cells: no difference with respect to cell type $F_{1,32}=2.13$, $P=0.154$ or cell type*dose interaction $F_{1,32}=1.06$, $P=0.31$, but a significant dose effect $F_{1,32}=36.7$, $P<0.001$). For the combined treatment, there was a dose-dependent increase in G1/G2 ratio (GLM, cell type, dose covariate and cell type*dose interaction terms all significant $F>16$, $P\leq0.001$) and data analysis for each cell line separately also showed a significant linear increase in G1/G2 ratio with increasing doses of fenretinide and bortezomib together (linear contrasts on one-way ANOVA, $F_{1,10}\geq8.7$, $P\leq0.014$).

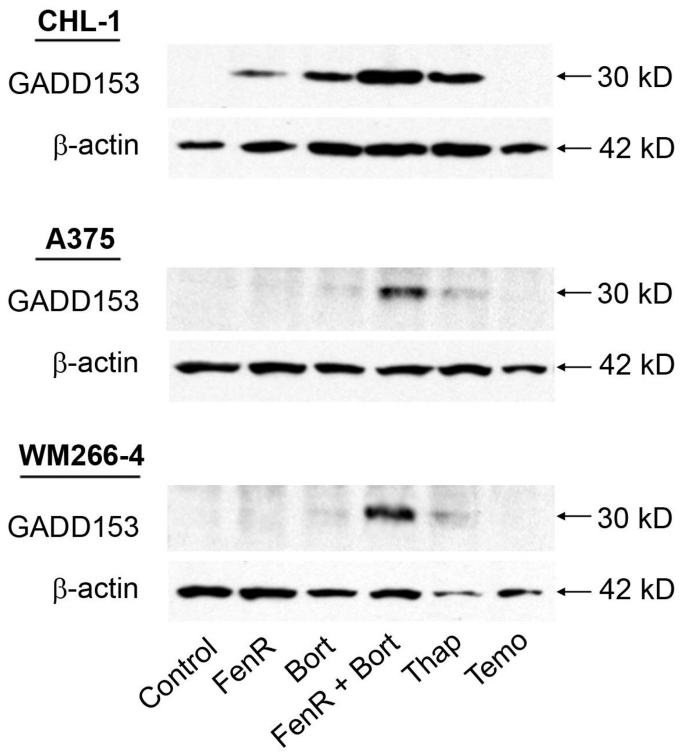

Figure 2.

Western blot analysis for the induction of GADD153 or β-actin (loading control) in CHL-1, A375 or WM266-4 cells after 18 h treatment with 10 μmol/L fenretinide (FenR), 0.2 μmol/L bortezomib (Bort), or combined treatment with both agents (10 μmol/L FenR and 0.2 μmol/L bortezomib [FenR + Bort]), in comparison to cells treated with either 7.5 μmol/L thapsigargin (Thap; a positive control for ER stress induction), 1 mmol/L temozolomide (Temo; an agent that induces apoptosis via DNA damage and not ER stress as a negative control) or control vehicle (Control).

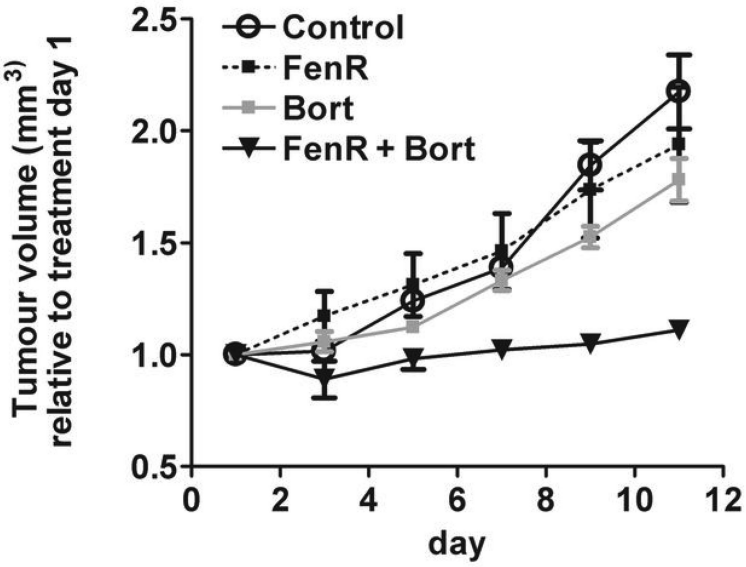

Figure 3.

Inhibition of tumor growth in xenograft tumors established from human A375 melanoma cells. Relative tumor volume after daily treatment with 1.45 mg/kg fenretinide (FenR), 0.1 mg/kg bortezomib (Bort) or both agents combined (FenR + Bort). Each point is the mean from 6 tumors ± SEM and is expressed relative to the tumor volume on day 1 of treatment. Ordinate, tumour volume (mm^3) relative to treatment on day 1; abscissa, day of treatment (day).

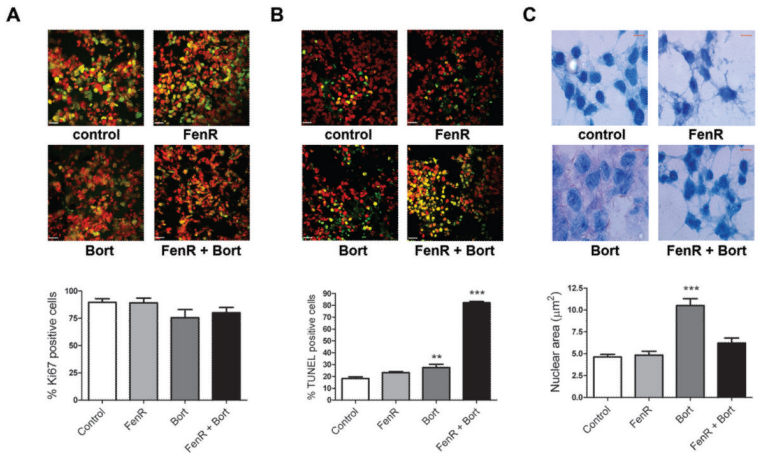

Figure 4.

Immunohistochemical analysis of A375 xenograft tumors treated with fenretinide and/or bortezomib. Panels *A*, *B* and *C* are micrographs of tumor sections stained with (*A*) Ki67, (*B*) TUNEL or (*C*) methylene blue, from animals treated for 10 days with 1.45 mg/kg fenretinide (FenR), 0.1 mg/kg bortezomib (Bort) or both agents together (FenR+Bort). In *A* and *B*, red is the TOTO-3 iodide counterstain, green is staining for Ki67 or TUNEL, respectively, and yellow is the signal from Ki67 or TUNEL staining on a cellular background. The bar graphs below each set of micrographs summarise the data analysis from tumor sections. For Ki67 (*A*) and TUNEL staining (*B*) each bar is the mean % + SEM of positive-stained cells (from at east 2100 cells from 3 independent staining runs) from 6 tumors in each treatment group. In the graph for *B*, ** indicates significantly different from control (Dunnett's; $P<0.01$) and *** indicates significantly different from control and bortezomib alone (Dunnett's and ANOVA contrast, $P<0.001$). For methylene blue staining (*C*), bar heights are the mean (6 tumors per treatment group) +SEM nuclear area (μm^2) of 200 nuclei from 4 independent staining experiments, in all cases assessed by two independent observers; *** indicates significantly different from control (Dunnett's, $P<0.001$); all other treatments were not significantly different from control. Scale bars represent 100 μm for Ki67 and TUNEL staining (white bars) and 5 μm for methylene blue staining (red bars).